

# ORGANOMETALLICS © Cite This: Organometallics 2019, 38, 2943–2952

Article

pubs.acs.org/Organometallics

# Synthesis and Characterization of (DIPPCCC)Fe Complexes: A Zwitterionic Metalation Method and CO<sub>2</sub> Reactivity

Bailey J. Jackson, Daniel C. Najera, Ellen M. Matson, Toby J. Woods, Jeffery A. Bertke, and Alison R. Fout\*®

School of Chemical Sciences, University of Illinois at Urbana—Champaign, 600 South Matthews Avenue, Urbana, Illinois 61801, United States

Supporting Information

**ABSTRACT:** The synthesis and characterization of a series of novel iron complexes has been accomplished using a monoanionic pincer bis(carbene) ligand framework. Metalation first proceeded through an isolated Fe(II) zwitterionic intermediate that was subsequently reduced in situ to Fe(0) to facilitate oxidative addition of the aryl C-H bond, generating the Fe<sup>II</sup>-H complexes. Varying the L-type ligand on these complexes exhibited profound effects, as observed by IR and

<sup>1</sup>H NMR spectroscopy. Higher oxidation states of Fe could also be supported in this ligand framework, as evidenced by the isolation of two Fe(III) complexes. Treating an Fe<sup>II</sup>-H complex with CO<sub>2</sub> generated an Fe-formate complex (κ<sup>2</sup>-OOCH) from insertion into the Fe<sup>II</sup>-H bond. The independent synthesis of this molecule was accomplished by treating Fe<sup>II</sup>-Cl with excess NaOOCH.

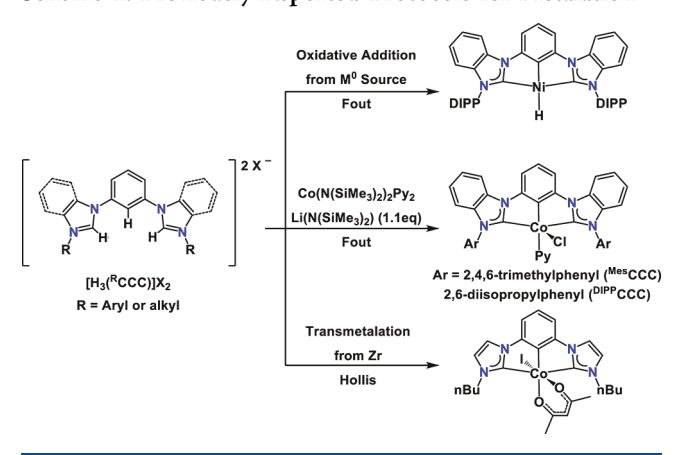
# INTRODUCTION

Pincer ligands have played a significant role in the development of new transition-metal catalysts. These tridentate, meridional frameworks are strong chelators and are easily modified, making them ideal supports for catalysts capable of a variety of transformations. 1-4 Research efforts continue to exploit ligand design to promote desired catalytic outcomes. For example, strong chelation to the metal center potentially minimizes catalyst degradation and electron-rich ligands (to engender low-spin states on a transition metal) and redoxactive ligands have been specifically developed to aid in multielectron reactivity on late first-row transition metals. Given the increased durability and activity demonstrated by Nheterocyclic carbene (NHC) ligated catalysts in comparison to their phosphine-based ligand counterparts, we sought a suitable pincer bis(carbene) ligand to stabilize complexes with iron.

Numerous NHC-based pincer complexes have been synthesized. However, bis(carbene) ligands featuring a phenyl linker on late first-row transition metals are underdeveloped. In fact, only our group and the Hollis group have demonstrated the ability to effectively install a late first-row transition metal into these types of systems. The limited number of examples highlights the difficulty that arises in attempts to metalate these systems, as activation of the backbone aryl C-H bond and both protons of the benzimidazolium salt is necessary. Various synthetic avenues have been employed for successful ligation of the ligand to a transition metal, including oxidative addition into the aryl C-H bond with  $Ni^0(COD)_2$  as the initial report of a first-row transition-metal CCC complex, 8a the direct use of metal-amide cobalt complexes, 8b and transmetalation with

zirconium reported by the Hollis group (Scheme 1).8c Interested in expanding this effort toward iron, we report a

Scheme 1. Previously Reported Protocols for Metalation



different synthetic route to access (DIPPCCC)Fe complexes (DIPPCCC = bis(diisoproplphenylbenzimidazol-2-ylidene)phenyl) which features an isolable zwitterionic intermediate. This metalation strategy resulted in the formation of iron-hydride complexes in high yield.

Received: April 25, 2019 Published: July 28, 2019



Scheme 2. Synthesis of Iron Complexes 1 and 2-L (L = PMe<sub>3</sub>, PPh<sub>3</sub>, Pyridine (Py))

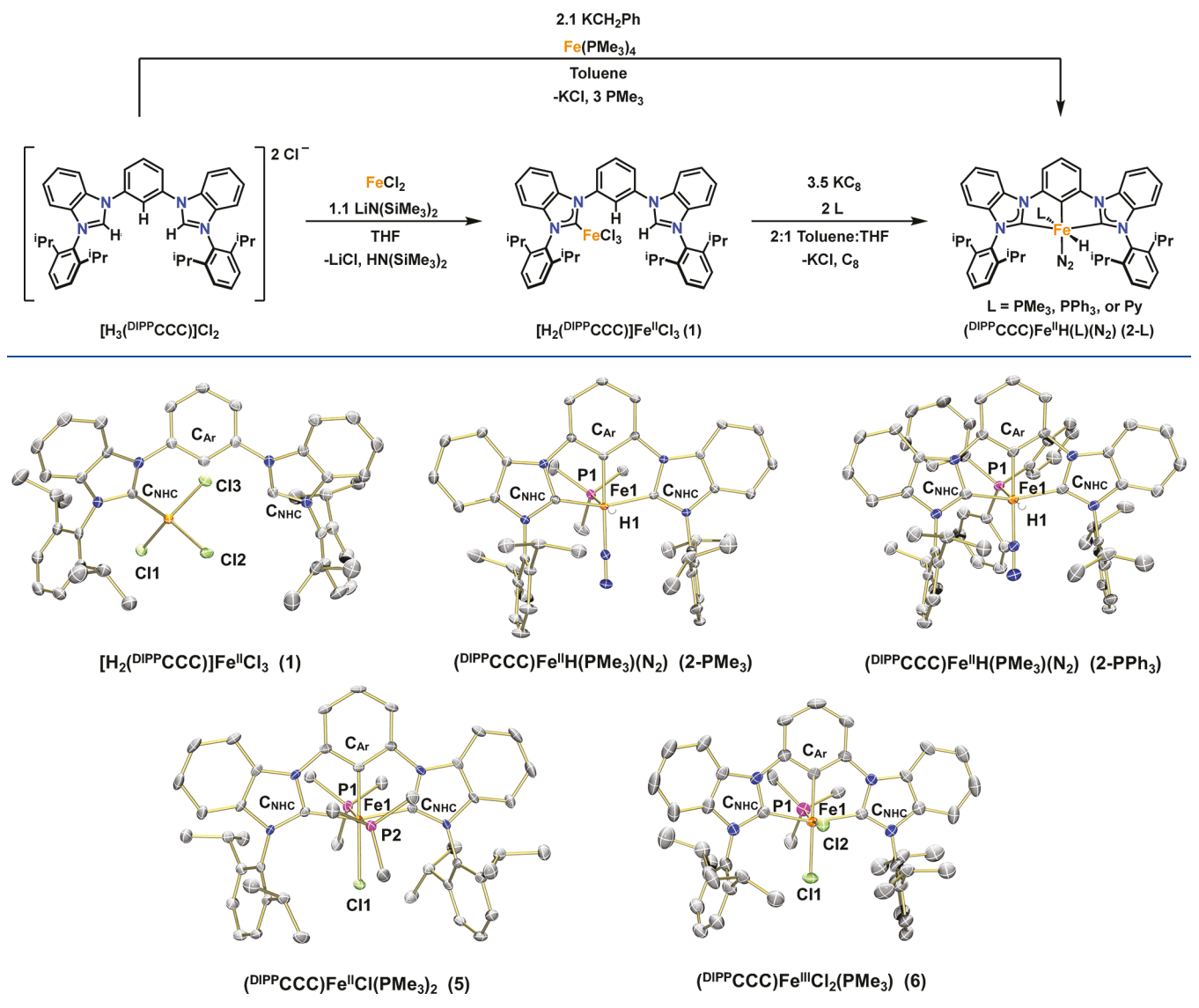


Figure 1. Molecular structures of 1, 2-PMe<sub>3</sub>, 2-PPh<sub>3</sub>, and 5 shown with 50% probability ellipsoids and that of 6a shown with 30% probability ellipsoids. Solvent molecules and selected hydrogen atoms have been omitted for clarity.

# RESULTS AND DISCUSSION

Synthesis of [H<sub>2</sub>(DIPPCCC)]Fe<sup>II</sup>Cl<sub>3</sub> (1). The initial exploration of metalation strategies like those previously described for cobalt or nickel with the DIPPCCC or MesCCC (MesCCC = bis(mesitylbenzimdazol-2-ylidene)phenyl) ligand did not afford the targeted (DIPPCCC)Fe products in appreciable yields when the analogous iron sources and reaction conditions were used. 8a,b Therefore, a different synthetic route to access the desired iron complexes was sought. Treatment of the benzimidazolium ligand salt with FeCl2 and 1 equiv of LiN(SiMe<sub>3</sub>)<sub>2</sub> in THF generates the zwitterionic complex [H<sub>2</sub>(DIPPCCC)]Fe<sup>II</sup>Cl<sub>3</sub> (1) in quantitative yields (Scheme 2). This compound displays a broadened, paramagnetic <sup>1</sup>H NMR spectrum. The solution magnetic moment of 1, as determined by the Evans method,  $^{10a}$  was found to be 5.73(5)  $\mu_{\rm B}$ , which is consistent with the calculated spin-orbit coupled magnetic moment of high-spin S = 2 tetrahedral Fe(II) complexes that typically range from 5.1 to 5.7  $\mu_{\rm B}$ . In order to gain a better understanding of the bonding in this complex, X-ray-quality

crystals of 1 were grown from DCM and hexanes at -35 °C (Figure 1). The Fe(II) center is bound to a single carbene ligand and three chlorides in a tetrahedral fashion with the remaining benzimidazolium moiety providing the charge balance.

**Synthesis of (DIPPCCC)Fe**<sup>II</sup>H(PMe<sub>3</sub>)(N<sub>2</sub>) (2-PMe<sub>3</sub>). After synthesizing the zwitterionic complex 1, we explored strategies to achieve the desired tridentate coordination of the ligand to the iron center. Accessing a zwitterionic intermediate for metalation has not been previously reported for monoanionic bis(carbene) pincer complexes. The synthesis of the singly coordinated NHC complexes with rhodium and iridium has been reported, but only with a metal to ligand ratio of 2:1.<sup>11</sup>

The addition of excess reductant (KC<sub>8</sub>, 3.5 equiv), base (LiN(SiMe<sub>3</sub>)<sub>2</sub>, 1.1 equiv), and trimethylphosphine (PMe<sub>3</sub>, 1 equiv) to complex **1** generates an Fe(0) intermediate in situ which oxidatively adds into the aryl C–H bond, affording ( $^{\text{DIPP}}$ CCC)Fe<sup>II</sup>H(PMe<sub>3</sub>)(N<sub>2</sub>) (**2**-PMe<sub>3</sub>) in quantitative yield (Scheme 2). This complex could also be generated, albeit in low yields (30%), by adding base (KCH<sub>2</sub>Ph, 2.1 equiv) and

Table 1. Selected IR and NMR Data for the Iron Hydride (
--

complex	IR $\nu_{\mathrm{L/L'}}~(\mathrm{cm^{-1}})$	IR $\nu_{\mathrm{Fe-H}}~(\mathrm{cm^{-1}})$	<sup>1</sup> H NMR (Fe-H, ppm)	<sup>31</sup> P NMR (ppm)	$J_{\mathrm{P-H}}$ (Hz)
2-PMe <sub>3</sub>	2099 (N <sub>2</sub> )	1722	-9.67 (d)	11	13
2-PPh <sub>3</sub>	$2099 (N_2)$	1791	-11.11 (d)	50	22.5
<b>2</b> -Py	2081 (N <sub>2</sub> )	1794	-18.70 (s)		
3-PMe <sub>3</sub> /CO	1948	1723	-10.96 (d)	10.5	4.5
3-PMe <sub>3</sub> / <sup>t</sup> BuNC	2016	1723	-10.45 (d)	14.9	5
4-CO	1983, 1927	1724	-8.41 (s)		
4- <sup>t</sup> BuNC	2047, 2002	1723	-8.87 (s)		

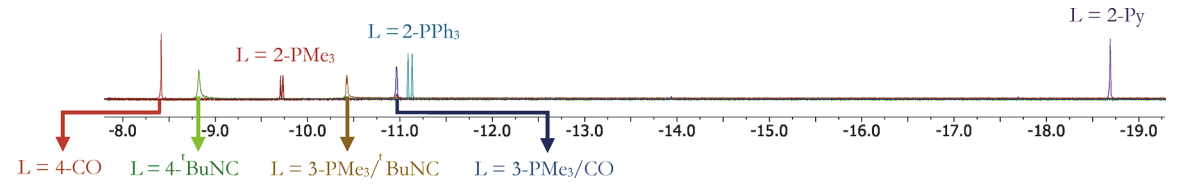


Figure 2. <sup>1</sup>H NMR spectra overlay of (DIPPCCC)Fe<sup>II</sup>H(L)(L'), upfield region only (C<sub>6</sub>D<sub>6</sub>, 25 °C).

Scheme 3. Synthesis of Iron Complexes 3-PMe<sub>3</sub>/CO, 3-PMe<sub>3</sub>/<sup>t</sup>BuNC, 4-CO, and 4-<sup>t</sup>BuNC

Fe(PMe<sub>3</sub>)<sub>4</sub> (1 equiv) to the benzimidazolium salt of the ligand. Vibrational frequencies for the Fe-H and N<sub>2</sub> were observed by solution IR spectroscopy at 1724 and 2102 cm<sup>-1</sup>, respectively, and by solid state ATR-IR at 1724 and 2099 cm<sup>-1</sup> (Table 1). Further characterization of 2-PMe<sub>3</sub> by <sup>1</sup>H NMR spectroscopy revealed a spectrum consistent with a C<sub>s</sub>-symmetric complex and featured a distinct doublet at -9.67 ppm assigned as the Fe-H ( $J_{P-H}$  = 13 Hz) resonance (Figure 2). Given the low coupling constant of less than 20 Hz, we tentatively assigned the PMe<sub>3</sub> bound cis to the hydride, as coupling constants for trans P-H coupling are typically much higher in magnitude  $(J_{P-H(trans)} = 90-150 \text{ Hz})$  than cis P-H coupling  $(J_{P-H(cis)} =$ 15-30 Hz). 12 However, a reversal in this trend has been observed by Guan and co-workers for (POCOP)Fe<sup>II</sup>H(PMe<sub>3</sub>)<sub>2</sub>  $(POCOP = 2,6-(R_2PO)_2C_6H_3; R = {}^{i}Pr, Ph, {}^{t}Bu)$  complexes, where  $J_{P-H(cis)} > J_{P-H(trans)}$ . Therefore, single-crystal diffraction studies were undertaken on 2-PMe3 to determine the actual conformation. These studies identified a distortedoctahedral geometry about iron with PMe3 trans to the hydride ligand and a bound N2 occupying the position trans to the CAr carbon of the pincer ligand (Figure 1). This is in opposition to our assignment based on P-H coupling constants, likely indicating a trend reversal similar to that observed by Guan and co-workers. 13 The Fe-H bond distance (1.52(2) Å) for 2-PMe<sub>3</sub> is within the expected range for Fe-H, and the N-N bond distance is relatively unactivated at 1.1078(17) Å. Meyer and co-workers have reported the only other example of tridentate coordination of a bis(carbene) ligand (NCC) to

iron. <sup>14</sup> Therefore, **2**-PMe<sub>3</sub> represents a rare example of a monoanionic bis(N-heterocyclic carbene) pincer iron complex with the ligand bound in a tridentate fashion.

With this new metalation strategy, which quantitatively generates  $H_2(^{\mathrm{DIPP}}CCC)Fe^{\mathrm{II}}Cl_3$  (1) and  $(^{\mathrm{DIPP}}CCC)Fe^{\mathrm{II}}H-(\mathrm{PMe_3})(\mathrm{N_2})$  (2-PMe<sub>3</sub>), the synthesis and characterization of a family of iron complexes featuring less Lewis basic ligands such as PPh<sub>3</sub> and pyridine (Py) was sought. Synthesis of  $(^{\mathrm{DIPP}}CCC)Fe^{\mathrm{II}}H(L)(L')$  ( $L=\mathrm{PPh_3}$ ,  $L'=\mathrm{N_2}$  (2-

 $PPh_3$ ); L = Py,  $L' = N_2$  (2-Py)). Following the previously established protocol, the addition of excess reductant (KC<sub>8</sub>, 3.5 equiv), base (LiN(SiMe<sub>3</sub>)<sub>2</sub>, 1.1 equiv), and PPh<sub>3</sub> or pyridine to 1 resulted in the formation of (DIPPCCC)Fe<sup>II</sup>H(PPh<sub>3</sub>)(N<sub>2</sub>) (2-PPh<sub>3</sub>) and (DIPPCCC)Fe<sup>II</sup>H(Py)(N<sub>2</sub>) (2-Py) in quantitative yields (Scheme 2). Both 2-PPh3 and 2-Py display <sup>1</sup>H NMR spectra simlar to that of 2-PMe3 with the most noticeable difference being the Fe-H resonance that shifts upfield from -9.67 ppm (2-PMe<sub>3</sub>) to -11.11 ppm (2-PPh<sub>3</sub>) and -18.70ppm (2-Py) (Figure 2 and Table 1). Like 2-PMe<sub>3</sub>, the hydride resonance for 2-PPh<sub>3</sub> is a doublet ( $J_{P-H} = 22.5 \text{ Hz}$ ) due to coupling of the hydride to the phosphine ligand. The similar J<sub>P-H</sub> coupling constant for 2-PPh<sub>3</sub>, in combination with steric considerations, indicates the same trans orientation of the ligated phosphine to the hydride as observed with 2-PMe<sub>3</sub>. Both 2-PMe<sub>3</sub> and 2-PPh<sub>3</sub> have ATR-IR N<sub>2</sub> stretches at 2099 cm<sup>-1</sup>, while 2-Py features a mildly red shifted N<sub>2</sub> stretch at 2081 cm<sup>-1</sup>. The ATR-IR spectra for 2-PPh<sub>3</sub> and 2-Py also include a blue-shifted Fe-H absorption ( $\nu_{\text{Fe-H}} = 1791$  and Organometallics Article Article

1794 cm<sup>-1</sup>, respectively) in comparison to 2-PMe<sub>3</sub> (1722 cm<sup>-1</sup>) (Table 1). Crystals suitable for X-ray diffraction studies were obtained from a concentrated hexanes solution of 2-PPh<sub>3</sub> at -35 °C. Akin to 2-PMe<sub>3</sub>, the iron center of 2-PPh<sub>3</sub> is in a distorted-octahedral geometry with PPh<sub>3</sub> trans to the hydride ligand and a bound N<sub>2</sub> occupying the position trans to the C<sub>Ar</sub> carbon of the pincer ligand (Figure 1). Analyses of the bond lengths for 2-PMe<sub>3</sub> and 2-PPh<sub>3</sub> indicate that these are within error of one another.

Though a variety of factors are likely contributing to the shifts of the hydride resonances in the  $^1\mathrm{H}$  NMR spectra,  $^{15}$  they roughly correlate to the  $\pi$ -acceptor strength of the L-type ligand. Although PPh3 is a better  $\pi$  acceptor than PMe3, the steric constraints afforded by PPh3 cause an upfield shift of the hydride resonance in comparison to 2-PMe3 (-11.11 ppm vs -9.67 ppm, respectively). These effects were further validated when 2-PMe3 and 2-PPh3 were compared to 2-Py; as pyridine is a poor  $\pi$  acceptor, the hydride resonance shifts further upfield to -18.70 ppm. This increase in hydridic character may also influence the thermal instability of 2-Py, as it decomposes in the solid state (and as a solution) over a few days if stored at room temperature.

Synthesis of  $(^{DIPP}CCC)Fe^{II}H(L)(L')$   $(L = L' = {}^{t}BuNC)$ (4- $^{t}$ BuNC); L = L' = CO (4-CO)). Interested in probing the Ltype ligand effects further, CO (1 atm) and excess <sup>t</sup>BuNC was added to 2-PMe<sub>3</sub> (Scheme 3). After monitoring by <sup>1</sup>H NMR spectroscopy for several hours, the kinetic products (DIPPCCC)Fe<sup>II</sup>H(PMe<sub>3</sub>)(CO) (3-PMe<sub>3</sub>/CO) and (DIPPCCC)-Fe<sup>II</sup>H(PMe<sub>3</sub>)(<sup>t</sup>BuNC) (3-PMe<sub>3</sub>/<sup>t</sup>BuNC) were identified. The N<sub>2</sub> stretch of 2-PMe<sub>3</sub> disappears and a new CO stretch at 1948 cm<sup>-1</sup> (free CO at 2143 cm<sup>-1</sup>) for 3-PMe<sub>3</sub>/CO can be observed. The N-C stretch of 3-PMe<sub>3</sub>/<sup>t</sup>BuNC appears at 2016 cm<sup>-1</sup> (free <sup>t</sup>BuNC 2138 cm<sup>-1</sup>) (Table 1). The <sup>1</sup>H NMR spectra for both complexes feature a slightly upfield shifted hydride doublet resonance at -10.96 ppm ( $J_{P-H} = 4.5$  Hz) for  $3-PMe_3/CO$  and -10.45 ppm ( $J_{P-H} = 5$  Hz) for 3-PMe<sub>3</sub>/<sup>t</sup>BuNC (Figure 1 and Table 1). The minimal change in the  $J_{P-H}$  coupling constants indicates no change in the phosphine-hydride conformation, and <sup>31</sup>P NMR spectroscopy also confirms retention of the PMe<sub>3</sub> ligand.

Monitoring the experiments in J. Young NMR tubes over 4 days by <sup>1</sup>H NMR spectroscopy reveals a collapse of the Fe-H resonance from a doublet to a singlet and a downfield shift of the Fe-H resonances to -8.41 and -8.87 ppm for the thermodynamic products (DIPPCCC)Fe<sup>II</sup>H(CO)<sub>2</sub> (4-CO) and (DIPPCCC)Fe<sup>II</sup>H(<sup>t</sup>BuNC)<sub>2</sub> (4-<sup>t</sup>BuNC), respectively (Scheme 3 and Figure 1). Analysis by IR spectroscopy also depicts two C-O stretches at 1983 and 1927 cm<sup>-1</sup> for 4-CO and two C-N stretches at 2047 and 2002 cm<sup>-1</sup> for 4-tBuNC, which are distinct from the previously characterized mixed ligand species (Table 1). Alternatively, complexes 4-CO and 4-tBuNC can also be synthesized by displacing the pyridine and N2 ligands from 2-Py with excess CO or \*BuNC in THF (Scheme 3). An immediate color change from purple to pale yellow is observed, and no mixed ligand species is seen when the reaction is monitored by <sup>1</sup>H NMR spectroscopy. Additionally, the release of the bound pyridine ligand can be tracked by <sup>1</sup>H NMR spectroscopy and generation of the desired complexes, 4-CO and 4-tBuNC, was accomplished in increased yields (92% and 96%, respectively).

Comparison of the Fe–H complexes may provide some insight into the electronics of our system. The overall trend observed is that the more  $\pi$  accepting the L-type ligands, the

more downfield the hydride resonance (i.e.,  $\rm CO > {}^{\rm t} \rm BuNC > PR_3 > pyridine$ ) (Figure 1). <sup>15</sup> The  $\rm C_{Ar}$  resonances in the <sup>13</sup>C NMR spectra of 2-L follow the same trend as the Fe–H resonances, shifting more downfield from 4-CO to 2-Py. IR spectroscopy also corroborates this observed pattern (Table 1). While these complexes follow the trend outlined above, recent studies have also indicated that the complexity and nonlinearity of spin–orbit coupling and diamagnetic and paramagnetic anisotropic contributions are also factors for the shifts in the Fe–H resonances. <sup>16</sup>

These contributions may help to explain the deviation in the trend for 3-PMe<sub>3</sub>/CO and 3-PMe<sub>3</sub>/tBuNC. Here an upfield shift of the hydride resonance is observed, instead of downfield, in the <sup>1</sup>H NMR spectra in spite of the replacement of the bound  $N_2$  with a more  $\pi$  accepting ligand. However, CO and BuNC are also more  $\sigma$  donating than  $N_2$ ; thus, a variety of factors could be contributing to this effect. The upfield shift is likely not due to ligand rearrangement in the mixed-ligand species 3-PMe<sub>3</sub>/CO and 3-PMe<sub>3</sub>/ $^{t}$ BuNC, since (a) the  $J_{P-H}$ coupling constants did not change significantly throughout the course of the reaction, (b) a significant downfield shift of the Fe-H resonance in the <sup>1</sup>H NMR spectra was not observed due to the binding of the new  $\pi$ -acceptor ligand trans to the hydride, and (c) no other intermediates were observed by <sup>1</sup>H NMR spectroscopy during the conversion of 3-PMe<sub>3</sub>/CO and 3-PMe<sub>3</sub>/<sup>t</sup>BuNC to 4-CO and 4-<sup>t</sup>BuNC, respectively.

Reactivity of (DIPPCCC)Fe<sup>II</sup>H(PMe<sub>3</sub>)(N<sub>2</sub>) (2-PMe<sub>3</sub>). The

Reactivity of (DIPPCCC)Fe<sup>II</sup>H(PMe<sub>3</sub>)(N<sub>2</sub>) (2-PMe<sub>3</sub>). The addition of HCl·Et<sub>2</sub>O (1 equiv) and PMe<sub>3</sub> (2 equiv) to 2-PMe<sub>3</sub> furnished (DIPPCCC)Fe<sup>II</sup>Cl(PMe<sub>3</sub>)<sub>2</sub> (5) in 90% yield, concomitant with the formation of H<sub>2</sub> (Scheme 4). Single-

Scheme 4. Synthesis of Iron Complexes 5 and 6a,b

crystal X-ray diffraction of **5** reveals an octahedral geometry around the Fe center with the chloride ligand bound trans to the  $C_{Ar}$  and two axial PMe<sub>3</sub> ligands (Figure 2). The  $^1H$  NMR spectrum and a single  $^{31}P$  NMR resonance (22.9 ppm) obtained for **5** are consistent with a  $C_s$ -symmetric complex. The  $^{13}C$  NMR  $C_{NHC}$  resonance appears at 225.91 ppm, while the  $C_{Ar}$  resonance appears at 189.69 ppm. Despite several attempts, the use of other noncoordinating acids to generate different Fe $^{II}$ -X complexes led to a myriad of products.

Previously we have observed the ability to access high-valent species for our CCC-ligated nickel and cobalt complexes species for our ccc-ligated nickel and cobalt complexes and are interested in accessing high-valent species with iron. Toward this end, treatment of 2-PMe<sub>3</sub> or 5 with one- and two-electron oxidants was undertaken. Unfortunately, the addition of two-electron oxidants did not lead to the isolation of any

Scheme 5. Synthesis of the Iron Complex (DIPPCCC)Fe<sup>II</sup>(K<sup>2</sup>-OOCH)(PMe<sub>3</sub>) (7)

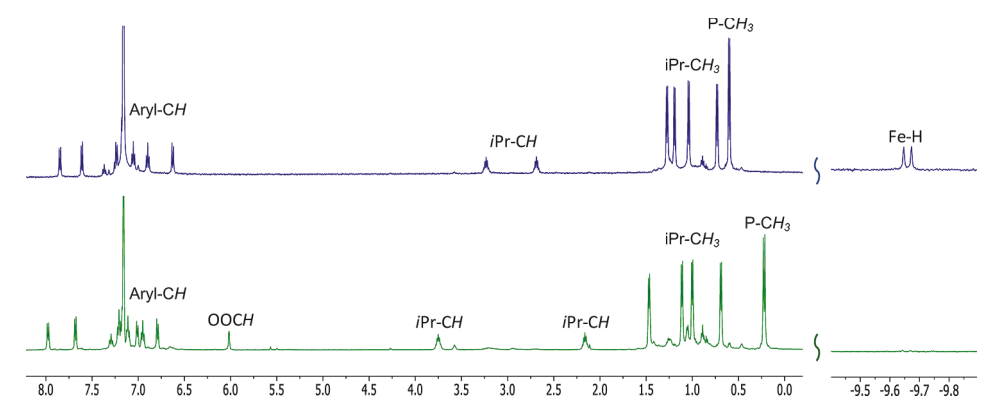


Figure 3. <sup>1</sup>H NMR spectra of 2-PMe<sub>3</sub> (top) and 7 (bottom) (C<sub>6</sub>D<sub>6</sub>, 25 °C).

Fe(IV) species. The addition of the one-electron oxidant ClCPh<sub>3</sub> to 2-PMe<sub>3</sub> or 5 led to only partial conversion to a new paramagnetic product by <sup>1</sup>H NMR spectroscopy. However, the addition of chloroform to 2-PMe<sub>3</sub> or 5 resulted in clean conversion to the same product, (DIPPCCC)Fe<sup>III</sup>Cl<sub>2</sub>(PMe<sub>3</sub>) (6a), in 90% yield with concomitant formation of dichloromethane, as observed in the <sup>1</sup>H NMR spectrum (Scheme 4). Complex 6a exhibits a paramagnetic <sup>1</sup>H NMR spectrum with resonances ranging from 100 to -20 ppm (Figure S14). Analysis of 6a by X-ray crystallography depicts a slightly distorted octahedral Fe center with the two chloride ligands cis to each other and Fe-Cl bond lengths of 2.362(3) Å (axial) and 2.264(3) Å (equatorial) (Figure 1). Alternatively, another high-valent iron complex, [(DIPPCCC)Fe<sup>III</sup>Cl(PMe<sub>3</sub>)<sub>2</sub>](PF<sub>6</sub>) (6b), could be generated upon the addition of AgPF<sub>6</sub> to complex 5 in dichloromethane (Scheme 4). <sup>1</sup>H NMR spectroscopy shows a paramagnetic spectrum similar to that of 6a, and a <sup>31</sup>P NMR resonance at 26.4 ppm indicates retention of the  $C_2$  symmetry of 5 (22.9 ppm). A <sup>31</sup>P NMR resonance at -143.5 ppm and two 19 F NMR resonances at -72.05 and -73.57 ppm show incorporation of the PF<sub>6</sub> anion (Figure S15).

**Reactivity of 2-PMe<sub>3</sub> with CO<sub>2</sub>.** Interested in exploring the reactivity of this iron-hydride complex, we targeted substrates that may insert into the Fe–H bond. The addition of 1 atm of  $CO_2(g)$  to 2-PMe<sub>3</sub> led to insertion of the  $CO_2$  into the Fe–H bond, resulting in formation of the iron–formate complex ( $^{DIPP}CCC$ )Fe<sup>II</sup>( $\kappa^2$ –OOCH)(PMe<sub>3</sub>) (7) (Scheme 5). This was evident by the loss of the hydridic resonance in the  $^1$ H NMR spectrum and the growth of a new resonance at 6.02 ppm for the formate proton (Figure 3). The  $^{31}$ P NMR spectrum indicates retention of the PMe<sub>3</sub> ligand with a singlet at 42.65 ppm, shifted significantly from that of 2-PMe<sub>3</sub> (11 ppm). Integration of the  $^1$ H NMR spectrum is consistent with a single PMe<sub>3</sub> ligand and no additional solvent molecules bound to the Fe center. This suggests either a five-coordinate Fe center or a multiatom-bound formate to achieve a

diamagnetic Fe(II) species. Analysis of 7 by IR spectroscopy is consistent with the loss of both the Fe-H and N<sub>2</sub> absorbances from 2-PMe3 and shows a new C-H stretch at 2815 cm<sup>-1</sup> for the bound formate ligand. The C-H IR absorbance falls within the region for known  $M-\kappa^2$ -OOCH complexes, although some  $M-\kappa^1$ -OOCH complexes have stretches in this same region. <sup>18</sup> Looking more closely at the fingerprint region reveals two stretches at 1562 cm<sup>-1</sup>. Peters and co-workers characterized a variety of Fe-formate complexes by IR spectroscopy and X-ray crystallography and found their Fe<sup>II</sup>( $\kappa^1$ -OOCH) complexes range from 1644 to 1603 cm<sup>-1</sup> while their Fe<sup>II</sup>( $\kappa^2$ -OOCH) complexes range from 1585 to 1553 cm<sup>-1</sup>. <sup>19</sup> Therefore, the most likely conformation of the product is  $(^{DIPP}CCC)Fe^{II}(\kappa^2\text{-OOCH})(PMe_3)$  (7) on the basis of these comparisons. Efforts to crystallographically characterize this new formate species were unsuccessful, and an independent synthesis was investigated instead. The independent synthesis of complex 7 was achieved via the addition of excess sodium formate to 5 (Scheme 5). Complex 5 could also be regenerated from 7 by adding HCl·Et<sub>2</sub>O and PMe<sub>3</sub> (Scheme 5).

# CONCLUSION

A host of iron complexes featuring the <sup>DIPP</sup>CCC monoanionic bis(carbene) pincer framework have been synthesized and characterized. Metalation in excellent yield was achieved via the isolation and further reduction of a zwitterionic Fe<sup>II</sup>–NHC complex. This method allowed for the isolation of several Fe<sup>II</sup>–H complexes with a host of different L-type ligands. Further oxidation of the Fe center was carried out using chloroform and AgPF<sub>6</sub> to give two different Fe(III) complexes. The reactivity of the Fe–H with CO<sub>2</sub> was investigated, and a ( $^{\rm DIPP}$ CCC)Fe<sup>II</sup>( $\kappa^2$ -OOCH)(PMe<sub>3</sub>) complex was identified by  $^{\rm I}$ H NMR and IR spectroscopy as well as independently synthesized from ( $^{\rm DIPP}$ CCC)Fe<sup>II</sup>Cl(PMe<sub>3</sub>)<sub>2</sub>. This family of iron complexes represents rare examples of iron ligated in a tridentate fashion with bis(carbene)aryl pincer ligands.

Organometallics Article Article

#### **■ EXPERIMENTAL SECTION**

General Considerations. All air- and moisture-sensitive manipulations were performed in an MBraun inert atmosphere drybox with an atmosphere of nitrogen. The MBraun drybox was equipped with one -35 °C freezer for cooling samples and crystallizations. Solvents for sensitive manipulations were dried and deoxygenated on a Glass Contour System (SG Water USA, Nashua, NH) and stored over 4 Å molecular sieves purchased from Strem following the literature procedure prior to use.<sup>20</sup> Iron(II) chloride anhydrous (98%) was purchased from Strem and used as received. Trimethylphosphine (1.0 M in THF), tert-butyl isocyanide (98%), hydrochloric acid (2.0 M in Et<sub>2</sub>O), and pyridine (99.8%) were purchased from Sigma-Aldrich and used as received. Triphenylphosphine (≥95% (GC)) was purchased from Sigma-Aldrich, recrystallized using ethanol, and dried before use. Lithium hexamethyldisilazide was purchased from Sigma-Aldrich and recrystallized under an inert atmosphere using toluene prior to use. Carbon monoxide (99.5%) and carbon dioxide (99.8%) were purchased from Specialty Gases of America and used as received. Iron(0) tetrakis(trimethylphosphine),<sup>13</sup> potassium graphite,<sup>21</sup> and the ligand  $[H_3(^{DIPP}CCC)]Cl_2(^{DIPP}CCC)$  = bis-(diisopropylphenylimidazol-2-ylidene)phenyl)<sup>8b</sup> were prepared according to literature procedures. Chloroform-d and benzene-d<sub>6</sub> were purchased from Cambridge Isotope Laboratories and were degassed and stored over 4 Å molecular sieves prior to use. Celite 545 (J. T. Baker) was dried in a Schlenk flask for 24 h under dynamic vacuum while heating to at least 150 °C prior to use in a glovebox.

<sup>1</sup>H, <sup>13</sup>C, and <sup>31</sup>P NMR spectra were recorded on a Varian spectrometer operating at 500 MHz (<sup>1</sup>H NMR), 126 MHz (<sup>13</sup>C NMR), and 202.4 MHz (<sup>31</sup>P NMR) at ambient temperature. All chemical shifts were reported relative to the peak of the residual solvent as a standard. Solid-state infrared spectra were recorded using a PerkinElmer Frontier FT-IR spectrophotometer equipped with a KRS5 thallium bromide/iodide Universal Attenuated Total Reflectance accessory. Solution-state infrared spectra were recorded using a PerkinElmer Frontier FT-IR spectrophotometer. Elemental analysis was performed by the University of Illinois at Urbana—Champaign School of Chemical Sciences Microanalysis Laboratory in Urbana. II.

School of Chemical Sciences Microanalysis Laboratory in Urbana, IL. **Preparation of H<sub>2</sub>(DIPPCCC)Fe<sup>II</sup>Cl<sub>3</sub> (1).** A 20 mL scintillation vial was charged with [H<sub>3</sub>(DIPPCCC)]Cl<sub>2</sub> (0.071 g, 0.101 mmol) and approximately 2 mL of THF. In two separate vials, 1 equiv of FeCl<sub>2</sub> (0.028 g, 0.049 mmol) and 1.1 equiv of Li(NSiMe<sub>3</sub>)<sub>2</sub> (0.019 g, 0.111 mmol) were dissolved in approximately 2 mL of THF each. The FeCl<sub>2</sub> was added to the off-white solution of the ligand, and the LiN(SiMe<sub>3</sub>)<sub>2</sub> was then added dropwise, resulting in an instantaneous color change to green-brown. After it was stirred for 3 h, the solution turned orange with a yellow precipitate. Solvents were removed under reduced pressure, and the yellow residue was dissolved in DCM, filtered over Celite, and the solvent again removed under reduced pressure. The product, H<sub>2</sub>(DIPPCCC)Fe<sup>II</sup>Cl<sub>3</sub>, was isolated as a yellow solid (0.08 g, 0.101 mmol, >99%). Crystals suitable for X-ray analysis were grown overnight from a concentrated solution of DCM and hexanes at -35 °C. Anal. Calcd for C44H47N4FeCl3·0.1CH2Cl2: C, 66.00; H, 5.93; N, 6.98. Found: C, 65.84; H, 5.90; N, 7.10. <sup>1</sup>H NMR (CDCl<sub>3</sub>, 500 MHz):  $\delta$  18.39, 17.67, 15.67, 15.53, 15.03, 13.71, 11.18,  $8.93,\ 8.52,\ 8.27,\ 7.48,\ 6.46,\ 6.13,\ 1.28,\ 0.89,\ -1.08,\ -1.22,\ -5.52,$ 

-8.20.  $\mu_{\rm eff} = 5.73(5)~\mu_{\rm B}$ . **Preparation of** (Pipp CCC)Fe<sup>II</sup>H(PMe<sub>3</sub>)(N<sub>2</sub>) (2-PMe<sub>3</sub>). A 20 mL scintillation vial was charged with H<sub>2</sub>(Pipp CCC)Fe<sup>II</sup>Cl<sub>3</sub> (1; 0.030 g, 0.038 mmol) and approximately 2 mL of toluene. A 1 equiv portion of PMe<sub>3</sub> (1.0 M THF, 0.04 mL, 0.038 mmol) was syringed into the vial. A 3.5 equiv amount of KC<sub>8</sub> (0.018 g, 0.133 mmol) was dissolved in 2 mL of THF. LiN(SiMe<sub>3</sub>)<sub>2</sub> (0.007 g, 0.042 mmol, 1.1 equiv) was dissolved in 1 mL of toluene. The LiN(SiMe<sub>3</sub>)<sub>2</sub> was placed in the vial of KC<sub>8</sub> and the mixture added dropwise to the iron solution. The reaction mixture was stirred at room temperature overnight, and the volatiles were removed under reduced pressure. Pentane (2 mL) was added to the solid and filtered over Celite; the filtrate was placed in the freezer at -35 °C to crystallize. Benzene was then added to the remaining solid and filtered over Celite until no further color washed down. The volatiles were removed under pressure from the filtrate, and the product as a vellow-red solid was obtained in good yield (0.026 mg, 0.033 mmol, 87%). After collection of the crystalline material from the pentane wash, the yield of product was quantitative. Crystals suitable for X-ray analysis were grown overnight at room temperature from a concentrated solution of pentane and toluene (20:1). Anal. Calcd for C<sub>47</sub>H<sub>55</sub>N<sub>6</sub>FeP·C<sub>4</sub>H<sub>8</sub>O·0.1CH<sub>2</sub>Cl<sub>2</sub>: C, 70.43; H, 7.31; N, 9.64. Found: C, 70.68; H, 6.93; N, 9.35. <sup>1</sup>H NMR (C<sub>6</sub>D<sub>6</sub>) 500 MHz):  $\delta$  –9.65 (d, J = 13 Hz, 1H, Fe-H), 0.60 (d, J = 7 Hz, 9H,  $P(CH_3)_3$ , 0.73 (d, J = 7 Hz, 6H, iPr-CH<sub>3</sub>), 1.04 (d, J = 7 Hz, 6H, iPr- $CH_3$ ), 1.20 (d, J = 7 Hz, 6H, iPr- $CH_3$ ), 1.27 (d, J = 7 Hz, 6H, iPr- $CH_3$ ), 2.68 (septet, J = 13 Hz, 2H, iPr-CH), 3.23 (septet, J = 13 Hz, 2H, iPr-CH), 6.6 (d, J = 7 Hz, 2H, Ar-CH), 6.89 (t, J = 7 Hz, 2H, Ar-CH), 7.05 (t, J = 7 Hz, 2H, Ar-CH), 7.18 (b, 4H, Ar-CH), 7.24 (d, J =7 Hz, 2H, Ar-CH), 7.37 (t, J = 7 Hz, 1H, Ar-CH), 7.62 (d, J = 7 Hz, 2H, Ar-CH), 7.84 (d, J = 7 Hz, 2H, Ar-CH). <sup>13</sup>C NMR (C<sub>6</sub>D<sub>6</sub>, 126 MHz):  $\delta$  149.09, 146.99, 146.48, 140.90, 135.06, 132.20, 129.98, 128.59, 125.27, 123.62, 122.00, 121.13, 120.39, 110.51, 109.68, 105.94, 28.68, 28.46, 25.65, 25.06, 24.64, 23.77, 15.73, 15.57. <sup>31</sup>P{<sup>1</sup>H} NMR ( $C_6D_6$ , 202.4 MHz):  $\delta$  11.02 (1P,  $P(CH_3)_3$ ). ATR-IR: 1723  $cm^{-1}$  (Fe-H), 2099  $cm^{-1}$  (N<sub>2</sub>). Solution-IR: 2102  $cm^{-1}$  (N<sub>2</sub>).

Alternate Preparation of (DIPPCCC)Fe<sup>II</sup>H(PMe<sub>3</sub>)(N<sub>2</sub>) (2-PMe<sub>3</sub>). A 20 mL scintillation vial was charged with [H<sub>3</sub>(DIPPCCC)]Cl<sub>2</sub> (0.028 g, 0.040 mmol) and approximately 4 mL of toluene. With vigorous stirring, 2.1 equiv of benzylpotassium (0.011 g, 0.084 mmol) was weighed by difference and added as an orange solid. After 1 h of stirring at room temperature, the solution was filtered over Celite and the filtrate was cooled to -35 °C. In a separate vial Fe(PMe<sub>3</sub>)<sub>4</sub> (0.014 g, 0.039 mmol) was dissolved in approximately 3 mL of pentane. The yellow solution was cooled to -35 °C. The filtrate, containing the free carbene H<sup>DIPP</sup>CCC generated in situ, was added dropwise to the iron(0) solution, resulting in a color change to brown. After 3 h of stirring at room temperature, volatiles were removed under reduced pressure. The brown-yellow residue was triturated with pentane, affording isolation of the product as a yellow solid (9.5 mg, 0.012 mmol, 30%).

Preparation of (DIPPCCC)Fe<sup>II</sup>H(PPh<sub>3</sub>)(N<sub>2</sub>) (2-PPh<sub>3</sub>). A 20 mL scintillation vial was charged with H<sub>2</sub>(DIPPCCC)Fe<sup>II</sup>Cl<sub>3</sub> (1; 0.030 g, 0.038 mmol) and approximately 2 mL of toluene. A 1 equiv portion of PPh<sub>3</sub> (0.010 g, 0.038 mmol) and 1.1 equiv of Li(N(SiMe<sub>3</sub>)<sub>2</sub>) (0.007 g, 0.042 mmol) were dissolved separately in 1 mL of toluene. A 3.5 equiv amount of KC<sub>8</sub> (0.018 g, 0.133 mmol) was dissolved in 2 mL of THF. The LiN(SiMe<sub>3</sub>)<sub>2</sub>) was added to the vial of KC<sub>8</sub> and the PPh<sub>3</sub> to the vial of the  $H_2(^{DIPP}CCC)Fe^{II}Cl_3$ . The LiN(SiMe<sub>3</sub>)<sub>2</sub>/KC<sub>8</sub> mixture was slowly added dropwise to the solution. The reaction mixture was stirred at room temperature overnight, and the volatiles were removed under reduced pressure. Pentane was added to the solid and filtered over Celite until no further color washed down. The volatiles were removed under pressure from the filtrate, and the product as an orange solid was obtained in quantitative yield (0.037 g, 0.038 mmol, >99%). Crystals suitable for X-ray analysis were grown overnight from a concentrated solution of hexanes at -35 °C. Anal. Calcd for C<sub>62</sub>H<sub>61</sub>N<sub>6</sub>FeP·0.5C<sub>4</sub>H<sub>8</sub>O·0.5CH<sub>2</sub>Cl<sub>2</sub>: C, 73.39; H, 6.30; N, 7.96. Found: C, 73.41; H, 6.04; N, 7.55. <sup>1</sup>H NMR (C<sub>6</sub>D<sub>6</sub>, 500 MHz):  $\delta$  –11.13 (d, J = 22.5 Hz, 1H, Fe-H), 0.70 (m, J = 7.5 Hz, 12H, iPr- $CH_3$ ), 0.90 (d, J = 6.5, 6H, iPr- $CH_3$ ), 1.10 (d, J = 7 Hz, 6H, iPr- $CH_3$ ), 2.53 (septet, J = 7 Hz, 2H, iPr-CH), 2.89 (septet, J = 7 Hz, 2H, iPr-CH), 6.57 (m, 6H, Ar-CH), 6.70 (t, J = 7.5 Hz, 2H, Ar-CH), 6.78 (t, J= 8.5 Hz, 4H, Ar-CH), 6.86 (t, J = 7.5 Hz, 2H, Ar-CH), 7.03 (m, 6H, Ar-CH), 7.27 (m, 6H, Ar-CH), 7.37 (d, J = 7.5 Hz, 2H, Ar-CH), 7.50 (t, J = 7.5 Hz, 2H, Ar-CH), 7.63 (d, J = 8 Hz, 2H, Ar-CH). <sup>13</sup>C NMR  $(C_6D_6, 126 \text{ MHz}): \delta 230.10, 183.01, 149.10, 147.74, 147.02, 141.43,$ 137.64, 135.80, 132.99, 132.91, 132.54, 129.90, 129.51, 127.07, 127.01, 125.27, 123.83, 121.80, 120.87, 120.78, 110.97, 109.84, 106.05, 29.38, 28.43, 25.50, 25.38, 24.26, 22.58. <sup>31</sup>P{<sup>1</sup>H} NMR  $(C_6D_6, 202.4 \text{ MHz}): \delta 50 \text{ (1P, } PPh_3). \text{ IR: } 1791 \text{ cm}^{-1} \text{ (Fe-H), } 2099$ 

Preparation of (DIPPCCC)Fe<sup>II</sup>H(Pyr)(N<sub>2</sub>) (2-Py). A 20 mL scintillation vial was charged with H<sub>2</sub>(DIPPCCC)Fe<sup>II</sup>Cl<sub>3</sub> (1; 0.030 g, 0.038 mmol) and approximately 2 mL of toluene. Excess pyridine (5

drops) was added to the vial and 1.1 equiv of LiN(SiMe<sub>3</sub>)<sub>2</sub> (0.007 g, 0.042 mmol) was dissolved in 2 mL of toluene. Three and a half equivalents of KC<sub>8</sub> (0.018 g, 0.133 mmol) was dissolved in 2 mL of THF. The LiN(SiMe<sub>3</sub>)<sub>2</sub> was added to the KC<sub>8</sub> and then slowly added dropwise to the reaction. The reaction was stirred at room temperature overnight and the volatiles removed under reduced pressure. Pentane was added to the solid and filtered over Celite until no further color was washed down. The filtrate was concentrated under reduced pressure and placed in the freezer at -35 °C to crystallize. The product as a purple crystalline material was obtained in good yield (0.027 mg, 0.034 mmol, 90%). Continued collection of crystalline material from the filtrate eventually gave a quantitative yield (0.029 g, 0.038 mmol, 99%). Anal. Calcd for C<sub>49</sub>H<sub>51</sub>FeN<sub>7</sub>·C<sub>7</sub>H<sub>8</sub>· 0.8C<sub>4</sub>H<sub>8</sub>O: C, 75.35; H, 6.99; N, 10.39. Found: C, 75.27; H, 6.64; N, 10.07. <sup>1</sup>H NMR ( $C_6D_6$ , 500 MHz):  $\delta$  –18.69 (s, 1H, Fe-H), 0.78 (d, J = 6.5 Hz, 6H, iPr-C $H_3$ ), 0.79 (d, J = 6.5 Hz, 6H, iPr-C $H_3$ ), 0.85 (d, J= 6.5 Hz, 6H, iPr-C $H_3$ ), 1.24 (d, J = 6.5 Hz, iPr-C $H_3$ ), 2.64 (septet, J= 7 Hz, 2H, iPr-CH), 2.84 (septet, J = 7 Hz, 2H, iPr-CH), 6.01 (d, J =6.5 Hz, 2H, Ar-CH), 6.40 (t, J = 7.5 Hz, 1H, Ar-CH), 6.63 (d, J = 7.5Hz, 2H, Ar-CH), 6.88 (d, J = 7.5 Hz, 2H, Ar-CH), 7.04 (t, J = 7.5 Hz, 2H, Ar-CH), 7.20 (d, J = 8 Hz, 2H, Ar-CH), 7.25 (d, J = 7.5 Hz, 2H, Ar-CH), 7.33 (t, J = 7.5 Hz, 2H, Ar-CH), 7.48 (t, J = 7.5 Hz, 1H, Ar-CH), 7.74 (d, J = 8 Hz, 2H, Ar-CH), 7.87 (d, J = 8 Hz, 2H, Ar-CH), 8.12 (d, J = 5.5 Hz, 2H, Ar-CH). <sup>13</sup>C NMR (C<sub>6</sub>D<sub>6</sub>, 126 MHz):  $\delta$ 229.28, 191.95, 154.47, 149.09, 148.69, 146.87, 140.49, 134.97, 132.70, 132.62, 130.06, 125.20, 123.80, 122.85, 122.00, 121.10, 120.96, 110.42, 109.78, 106.59, 28.64, 28.56, 26.14, 25.21, 24.29, 23.35. IR: 1794 cm<sup>-1</sup> (Fe-H), 2081 cm<sup>-1</sup> (N<sub>2</sub>).

Preparation of (DIPPCCC)Fe<sup>II</sup>H(CO)<sub>2</sub> (4-CO). A 50 mL Schlenk flask was charged with (DIPPCCC)Fe<sup>II</sup>H(PMe<sub>3</sub>)(N<sub>2</sub>) (2-PMe<sub>3</sub>) (0.020 g, 0.025 mmol) and approximately 5 mL of benzene. CO gas (4 atm) was added to the flask after freeze-pump-thawing. The reaction mixture was stirred at room temperature over several days and turned slowly from red to pale yellow, and the volatiles were removed under reduced pressure. The product (DIPPCCC)Fe<sup>II</sup>H(CO)<sub>2</sub> was obtained as a pale yellow solid in high yield (0.015 g, 0.02 mmol, 80%). Anal. Calcd for C<sub>46</sub>H<sub>46</sub>N<sub>4</sub>O<sub>2</sub>Fe·0.3CH<sub>2</sub>Cl<sub>2</sub>: C, 72.39; H, 6.11; N, 7.29. Found: C, 72.65; H, 5.96; N, 7.36. <sup>1</sup>H NMR ( $C_6D_6$ , 500 MHz):  $\delta$ -8.42 (s, 1H, Fe-H), 0.77 (d, J = 6.5 Hz, 6H, iPr-CH<sub>3</sub>), 0.87 (d, J = 7Hz, 6H, iPr-C $H_3$ ), 1.13 (d, J = 6.5 Hz, 6H, iPr-C $H_3$ ), 1.44 (d, J = 6.5Hz, 6H, iPr- $CH_3$ ), 2.36 (septet, J = 7 Hz, 2H, iPr-CH), 2.98 (septet, J= 7 Hz, 2H, iPr-CH), 6.57 (d, J = 8 Hz, 2H, Ar-CH), 6.86 (t, J = 7.5Hz, 2H, Ar-CH), 7.04 (t, J = 7.5 Hz, 2H, Ar-CH), 7.10 (d, J = 8 Hz, 2H, Ar-CH), 7.18 (m, 2H, Ar-CH) 7.23 (d, J = 8 Hz, 2H, Ar-CH), 7.43 (t, J = 8 Hz, 1H, Ar-CH), 7.61 (d, J = 8 Hz, 2H, Ar-CH), 7.72 (d, J = 8 Hz, 2H, Ar-CH). <sup>13</sup>C NMR (C<sub>6</sub>D<sub>6</sub>, 126 MHz):  $\delta$  220.05, 214.04, 209.82, 174.82, 147.81, 147.66, 146.91, 139.20, 133.57, 131.84, 130.63, 124.85, 124.49, 122.93, 122.88, 122.19, 111.07, 110.86, 108.16, 28.78, 28.60, 25.85, 24.84, 23.84, 23.54. IR: 1983, 1927 cm<sup>-1</sup>

Alternate Preparation of (DIPPCCC)Fe<sup>II</sup>H(CO)<sub>2</sub> (4-CO). A 50 mL Schlenk flask was charged with (DIPPCCC)Fe<sup>II</sup>H(Pyr)(N<sub>2</sub>) (2-Py; 0.020 g, 0.025 mmol) and approximately 5 mL of benzene. CO gas (4 atm) was added to the flask after freeze-pump-thawing. The reaction mixture immediately changed from purple to pale yellow. The volatiles were removed under reduced pressure. The product (DIPPCCC)Fe<sup>II</sup>H(CO)<sub>2</sub> was obtained as a pale yellow solid in high yield (0.017 mg, 0.023 mmol, 92%).

Preparation of (DIPPCCC)Fe<sup>II</sup>H('BuNC)<sub>2</sub> (4-'BuNC). A 20 mL scintillation vial was charged with (DIPPCCC)Fe<sup>II</sup>H(PMe<sub>3</sub>)(N<sub>2</sub>) (2-PMe<sub>3</sub>; 0.020 g, 0.025 mmol) and approximately 5 mL of THF. Excess tert-butyl isocyanide (Seq, 0.014 mL, 0.125 mmol) was added to the vial. The reaction mixture was stirred at room temperature over several days and turned slowly from orange to yellow-green. The volatiles were removed under reduced pressure, and the product (DIPPCCC)Fe<sup>II</sup>H('BuNC)<sub>2</sub> was obtained as a pale yellow solid in high yield (0.018 g, 0.021 mmol, 84%). Anal. Calcd for C<sub>54</sub>H<sub>64</sub>N<sub>6</sub>Fe·0.3CH<sub>2</sub>Cl<sub>2</sub>: C, 74.24; H, 7.41; N, 9.57. Found: C, 74.36; H, 7.27; N, 9.21. <sup>1</sup>H NMR (C<sub>6</sub>D<sub>6</sub>, 500 MHz): δ –8.82 (s, 1H, Fe-H), 0.61 (s, 9H, 'Bu-(CH<sub>3</sub>)<sub>3</sub>), 0.62 (s, 9H, 'Bu-(CH<sub>3</sub>)<sub>3</sub>), 0.82 (d, J = 6.5 Hz, 6H, iPr-

CH<sub>3</sub>), 1.03 (d, J = 7 Hz, 6H, iPr-CH<sub>3</sub>), 1.31 (d, J = 6.5 Hz, 6H, iPr-CH<sub>3</sub>), 1.51 (d, J = 7 Hz, 6H, iPr-CH<sub>3</sub>), 2.87 (septet, J = 7 Hz, 2H, iPr-CH), 3.34 (septet, J = 7 Hz, 2H, iPr-CH), 6.27 (d, J = 8 Hz, 2H, Ar-CH), 6.84 (t, J = 7.5 Hz, 2H, Ar-CH), 7.04 (t, J = 7.5 Hz, 2H, Ar-CH), 7.19 (d, J = 8 Hz, 2H, Ar-CH), 7.25 (d, J = 7.5 Hz, 2H, Ar-CH), 7.31 (t, J = 7.5 Hz, 2H, Ar-CH), 7.53 (t, J = 8 Hz, 1H, Ar-CH), 7.84 (d, J = 7.5 Hz, 2H, Ar-CH), 7.97 (d, J = 8 Hz, 2H, Ar-CH). <sup>13</sup>C NMR (C<sub>6</sub>D<sub>6</sub>, 126 MHz): δ 228.03, 187.33, 186.39, 175.31, 148.70, 147.96, 146.97, 140.85, 136.53, 132.06, 129.48, 125.14, 124.80, 122.10, 120.98, 120.02, 109.60, 109.49, 106.00, 55.39, 54.15, 31.27, 31.17, 28.69, 28.53, 25.14, 24.94, 24.59, 23.74. IR: 2047, 2002 cm<sup>-1</sup> (C-N).

Alternate Preparation of (OIPPCCC)Fe<sup>II</sup>H('BuNC)<sub>2</sub> (4-'BuNC). A 20 mL scintillation vial was charged with (DIPPCCC)Fe<sup>II</sup>H(Pyr)(N<sub>2</sub>) (2-Py; 0.020 g, 0.025 mmol) and approximately 5 mL of THF. Excess tert-butyl isocyanide (3 equiv, 0.008 mL, 0.075 mmol) was added to the vial. The reaction mixture immediately changed from purple to yellow-green. The volatiles were removed under reduced pressure, and the product (DIPPCCC)Fe<sup>II</sup>H('BuNC)<sub>2</sub> was obtained as a pale yellow solid in high yield (0.021 mg, 0.024 mmol, 96%).

yellow solid in high yield (0.021 mg, 0.024 mmol, 96%).

Preparation of (DIPPCCC)Fe<sup>II</sup>CI(PMe<sub>3</sub>)<sub>2</sub> (5). A 20 mL scintillation vial was charged with (DIPPCCC)Fe<sup>II</sup>H(PMe<sub>3</sub>)(N<sub>2</sub>) (2-PMe<sub>3</sub>; 0.020 g, 0.025 mmol) and approximately 3 mL of THF. With vigorous stirring, 2 equiv of PMe<sub>3</sub> (1.0 M THF, 0.05 mL, 0.05 mmol) was syringed into the vial followed by 1.1 equiv of HCl·Et<sub>2</sub>O (2.0 M Et<sub>2</sub>O, 0.014 mL, 0.0275 mmol), resulting in a dark red solution. The solution was stirred overnight at room temperature, and the volatiles were removed under reduced pressure, giving the pure product (0.020 g, 0.023 mmol, 92%). Crystals suitable for X-ray analysis were grown from DCM. Anal. Calcd for C<sub>50</sub>H<sub>63</sub>N<sub>4</sub>FeClP<sub>2</sub>·0.8CH<sub>2</sub>Cl<sub>2</sub>: C, 64.82; H, 6.92; N, 5.95. Found: C, 64.55; H, 6.69; N, 6.38. <sup>1</sup>H NMR (C<sub>6</sub>D<sub>6</sub>, 500 MHz):  $\delta$  0.47 (s, 18H, (P(CH<sub>3</sub>)<sub>3</sub>)2), 0.90 (d, J = 6.6 Hz, 12H,  $iPr-CH_3$ ), 1.26 (d, I = 6.5 Hz, 12H,  $iPr-CH_3$ ), 2.95 (septet, I = 6.5 Hz, 4H, iPr-CH), 6.73 (d, J = 8 Hz, 2H, Ar-CH), 6.88 (t, J = 7.5 Hz, 2H, Ar-CH), 7.07 (t, J = 7.6 Hz, 2H, Ar-CH), 7.20 (d, J = 7.8 Hz, 4H, Ar-CH), 7.24 (t, J = 6.5 Hz, 2H, Ar-CH), 7.33 (t, J = 7 Hz, 1H, Ar-CH), 7.63 (d, J = 7.7 Hz, 2H, Ar-CH), 7.91 (d, J = 8 Hz, 2H, Ar-CH). <sup>13</sup>C NMR ( $C_6D_6$ , 126 MHz):  $\delta$  225.91, 189.69, 149.52, 147.67, 141.94, 135.62, 132.10, 129.79, 124.32, 122.23, 121.15, 118.60, 112.79, 109.29, 106.79, 29.21, 26.48, 23.69, 16.57.  ${}^{31}P\{{}^{1}H\}$  NMR ( $C_6D_{61}$ 

202.4 MHz): δ 22.90 (1P,  $P(CH_3)_3$ ).

Preparation of (DIPPCCC)Fe<sup>III</sup>(CI)<sub>2</sub>(PMe<sub>3</sub>) (6a). A 20 mL scintillation vial was charged with (DIPPCCC)Fe<sup>II</sup>Cl(PMe<sub>3</sub>)<sub>2</sub> (5; 0.020 g, 0.0229 mmol) or (DIPPCCC)Fe<sup>II</sup>H(PMe<sub>3</sub>)(N<sub>2</sub>) (2-PMe<sub>3</sub>; 0.020 g 0.025 mmol), excess chloroform (CHCl<sub>3</sub>) was added, and the mixture was stirred at room temperature for 20 min. The red solid changed to a dark green solution. The volatiles were then removed under reduced pressure to yield the pure product (0.017 g, 0.021 mmol, 92%). Crystals suitable for X-ray analysis were grown from DCM and pentane. Anal. Calcd for C<sub>47</sub>H<sub>54</sub>N<sub>4</sub>FeCl<sub>2</sub>P·1.35CH<sub>2</sub>Cl<sub>2</sub>: C, 61.3; H, 6.03; N, 5.91. Found: C, 61.3; H, 5.68; N, 5.96. <sup>1</sup>H NMR (CDCl<sub>3</sub>, 500 MHz): δ –19.35, –2.92, –1.19, 0.42, 1.09, 1.22, 1.41, 1.54, 2.37, 2.70, 6.44, 6.88, 7.40, 7.60, 8.56, 8.91, 11.21, 15.69, 20.49, 80.17, 100.51.  $\mu_{\text{eff}} = 2.81 \ \mu_{\text{B}}$ .

Preparation of [(DIPPCCC)Fe<sup>III</sup>CI(PMe<sub>3</sub>)<sub>2</sub>](PF<sub>6</sub>) (6b). A 20 mL scintillation vial was charged with (DIPPCCC)Fe<sup>II</sup>Cl(PMe<sub>3</sub>)<sub>2</sub> (2-PMe; 0.020 g, 0.0229 mmol) and approximately 3 mL of THF. Silver hexafluorophosphate (0.058 g, 0.0229 mmol) was dissolved in a separate vial in 2 mL of THF and added to the solution dropwise. The solution was stirred at room temperature overnight, and the red solution changed to dark green with a precipitate, which was filtered off through Celite. The volatiles were removed under reduced pressure, yielding the product, which was recrystallized by a slow diffusion of pentane into DCM (0.022 g, 0.022 mmol, 95%). Anal. Calcd for C<sub>50</sub>H<sub>63</sub>N<sub>4</sub>FeClP<sub>3</sub>F<sub>6</sub>·0.2CH<sub>2</sub>Cl<sub>2</sub>: C, 58.24; H, 6.17; N, 5.41. Found: C, 58.36; H, 6.36; N, 5.29.  $^{1}$ H NMR (C<sub>6</sub>D<sub>6</sub>, 21  $^{\circ}$ C):  $\delta$ -19.52, -3.01, -1.24, 1.25, 1.88, 2.19, 4.50, 6.40, 7.53, 8.11, 8.49, 8.85, 10.91, 14.92, 19.52.  ${}^{31}P{}^{1}H$  NMR ( $C_6D_6$ , 21  ${}^{\circ}C$ ):  $\delta$  26.40 (1P,  $P(CH_3)_2$ ), -143.50 (1P, PF<sub>6</sub>). <sup>19</sup>F{<sup>1</sup>H} NMR (C<sub>6</sub>D<sub>6</sub>, 21 °C):  $\delta$ -72.05, -73.57 (PF<sub>6</sub>).

Preparation of (DIPPCCC)Fe<sup>II</sup>( $\kappa^2$ -OOCH)(PMe<sub>3</sub>) (7). A 50 mL Schlenk flask was charged with (DIPPCCC)Fe<sup>II</sup>H(PMe<sub>3</sub>)(N<sub>2</sub>) (2-PMe<sub>3</sub>; 0.020 g, 0.025 mmol) and approximately 3 mL of benzene. The reaction mixture was stirred at room temperature under an atmosphere of CO<sub>2</sub> for 36 h. The volatiles were removed under reduced pressure, and the product, (DIPPCCC)Fe<sup>II</sup>( $\kappa^2$ -OOCH)-(PMe<sub>3</sub>), was obtained as a red-purple solid. Pentane was added, the solution was filtered over Celite, and the filtrate was placed in the freezer at -35 °C to crystallize. Red-purple needle crystals were obtained in 60% yield (0.012 g, 0.015 mmol). Concentrating the filtrate a second time yielded more red-purple crystals. <sup>1</sup>H NMR  $(C_6D_6, 21 \text{ °C})$ :  $\delta 0.22 \text{ (d, } J = 8.5 \text{ Hz, } 9H, (P(CH_3)_3)_2), 0.69 \text{ (d, } J =$ 6.5 Hz, 6H, iPr-C $H_3$ ), 1.00 (d, J = 7 Hz, 6H, iPr-C $H_3$ ), 1.11 (d, J = 76.5 Hz, 6H, iPr-C $H_3$ ), 1.47 (d, J = 7 Hz, 6H, iPr-C $H_3$ ), 2.16 (septet, J= 6.5 Hz, 2H, iPr-CH), 3.75 (septet, I = 7 Hz, 2H, iPr-CH), 6.02 (d, I= 4 Hz, 1H, OOCH), 6.79 (d, J = 8 Hz, 2H, Ar-CH), 6.95 (t, J = 7.5Hz, 2H, Ar-CH), 7.01 (d, J = 7.5 Hz, 2H, Ar-CH), 7.11 (t, J = 8 Hz, 2H, Ar-CH), 7.18 (m, 2H, Ar-CH) 7.21 (t, J = 7.5 Hz, 2H, Ar-CH), 7.30 (t, J = 8 Hz, 1H, Ar-CH), 7.68 (d, J = 7.5 Hz, 2H, Ar-CH), 7.98 (d, J = 8 Hz, 2H, Ar-CH).  $^{31}P\{^{1}H\}$  NMR ( $C_6D_6$ , 202.4 MHz): 42.65 (1P, P(CH<sub>3</sub>)<sub>3</sub>). IR: 2815 cm<sup>-1</sup> (OOCH), 1562 cm<sup>-1</sup> (OOCH), 1276 cm<sup>-1</sup> (OOCH). Decarboxylation of 7 to 2-PMe<sub>3</sub> precluded characterization by <sup>13</sup>C NMR spectroscopy and CHN analysis.

Alternate Preparation of (DIPPCCC)Fe<sup>II</sup>( $\kappa^2$ -OOCH)(PMe<sub>3</sub>). A 20

Alternate Preparation of (DIPPCCC)Fe<sup>II</sup>(κ²-OOCH)(PMe<sub>3</sub>). A 20 mL scintillation vial was charged with (DIPPCCC)Fe<sup>II</sup>Cl(PMe<sub>3</sub>)<sub>2</sub> (5; 0.020 g, 0.023 mmol) and approximately 5 mL of THF. Excess sodium formate (10 equiv, 0.016 g, 0.23 mmol) was placed in the vial. The reaction mixture was stirred at room temperature for 4 days, changing from red-orange to purple. The volatiles were removed under reduced pressure. Pentane was added, and the solution was filtered over Celite. The volatiles were removed under reduced pressure, and the product, (DIPPCCC)Fe<sup>II</sup>(κ²-OOCH)(PMe<sub>3</sub>), was obtained as a red-purple solid (0.012 g, 0.015 mmol, 64%).

#### ASSOCIATED CONTENT

# **S** Supporting Information

The Supporting Information is available free of charge on the ACS Publications website at DOI: 10.1021/acs.organomet.9b00271.

Experimental spectra and crystallographic data (PDF)

#### **Accession Codes**

CCDC 1912013–1912017 contain the supplementary crystallographic data for this paper. These data can be obtained free of charge via www.ccdc.cam.ac.uk/data\_request/cif, or by emailing data\_request@ccdc.cam.ac.uk, or by contacting The Cambridge Crystallographic Data Centre, 12 Union Road, Cambridge CB2 1EZ, UK; fax: +44 1223 336033.

# AUTHOR INFORMATION

### **Corresponding Author**

\*E-mail for A.R.F.: fout@illinois.edu.

ORCID

Toby J. Woods: 0000-0002-1737-811X Alison R. Fout: 0000-0002-4669-5835

**Notes** 

The authors declare no competing financial interest.

# ACKNOWLEDGMENTS

The authors thank the NSF for financial support with a CAREER award (1351961) to A.R.F. The authors also thank Yu-Sheng Chen and ChemMatCARS Sector 15, which is supported by the Divisions of Chemistry (CHE) and Materials Research (DMR), National Science Foundation, under grant number NSF/CHE- 1834750. The Advanced Photon Source,

an Office of Science User Facility operated for the U.S. Department of Energy (DOE) Office of Science by Argonne National Laboratory, supported by the U.S. DOE under contract No. DE-AC02-06CH11357, was used for aiding in the collection of 2-PPh<sub>3</sub>.

### REFERENCES

(1) (a) Silantyev, G. A.; Förster, M.; Schluschaß, B.; Abbenseth, J.; Würtele, C.; Volkmann, C.; Holthausen, M. C.; Schneider, S. Dinitrogen Splitting Coupled to Protonation. Angew. Chem., Int. Ed. 2017, 56, 5872-5876. (b) Tanaka, H.; Nishibayashi, Y.; Yoshizawa, K. Interplay between Theory and Experiment for Ammonia Synthesis Catalyzed by Transition Metal Complexes. Acc. Chem. Res. 2016, 49, 987-995. (c) Klopsch, I.; Kinauer, M.; Finger, M.; Würtele, C.; Schneider, S. Conversion of Dinitrogen into Acetonitrile under Ambient Conditions. Angew. Chem., Int. Ed. 2016, 55, 4786-4789. (d) Hölscher, M.; Prechtl, M. H. G.; Leitner, W. Can [M(H)2(H2)-(PXP)] Pincer Complexes (M = Fe, Ru, Os; X = N, O, S) Serve as Catalyst Lead Structures for NH3 Synthesis from N2 and H2? Chem. -Eur. J. 2007, 13, 6636-6643. (e) Bezdek, M. J.; Chirik, P. J. Expanding Boundaries: N 2 Cleavage and Functionalization beyond Early Transition Metals. Angew. Chem., Int. Ed. 2016, 55, 7892-7896. (f) Eizawa, A.; Arashiba, K.; Tanaka, H.; Kuriyama, S.; Matsuo, Y.; Nakajima, K.; Yoshizawa, K.; Nishibayashi, Y. Remarkable Catalytic Activity of Dinitrogen-Bridged Dimolybdenum Complexes Bearing NHC-Based PCP-Pincer Ligands toward Nitrogen Fixation. Nat. Commun. 2017, 8, 14874.

(2) (a) Szabó, K. J. Pincer and Pincer-Type Complexes: Applications in Organic Synthesis and Catalysis, 1st ed.; Wiley-VCH: 2014. (b) Someya, C. I.; Irran, E.; Enthaler, S. Synthesis of Ni(II) Complexes with Unsymmetric [O,N,O']-Pincer Ligands and Their Use as Precatalysts in Carbon-Carbon Bond Formations to Access Diarylmethanes. Inorg. Chim. Acta 2014, 421, 136-144. (c) Kose, O.; Saito, S. Cross-Coupling Reaction of Alcohols for Carbon-Carbon Bond Formation Using Pincer-Type NHC/Palladium Catalysts. Org. Biomol. Chem. 2010, 8, 896-900. (d) Aydin, J.; Szabó, K. J. Palladium-Pincer Complex Catalyzed C-C Coupling of Allyl Nitriles with Tosyl Imines via Regioselective Allylic C-H Bond Functionalization. Org. Lett. 2008, 10, 2881-2884. (e) Csok, Z.; Vechorkin, O.; Harkins, S. B.; Scopelliti, R.; Hu, X. Nickel Complexes of a Pincer NN 2 Ligand: Multiple Carbon-Chloride Activation of CH<sub>2</sub>Cl<sub>2</sub> and CHCl<sub>3</sub> Leads to Selective Carbon-Carbon Bond Formation. J. Am. Chem. Soc. 2008, 130, 8156-8157. (f) Frech, C. M.; Shimon, L. J. W.; Milstein, D. Methylene Transfer from SnMe Groups Mediated by a Rhodium(I) Pincer Complex: Sn—C, C—C, and C—H Bond Activation. Chem. -Eur. J. 2007, 13, 7501-7509. (g) Soro, B.; Stoccoro, S.; Minghetti, G.; Zucca, A.; Cinellu, M. A.; Manassero, M.; Gladiali, S. The First Pincer-Aryl [M-(NCN)] Complexes {M = Pd(II); Pt(II)} with Chiral Pyridine Donors: Synthesis and Catalytic Activity in C-C Bond Formation. Inorg. Chim. Acta 2006, 359, 1879-1888. (h) Fossey, J. S.; Richards, C. J. A Direct Route to Platinum NCN-Pincer Complexes Derived from 1,3- Bis(Imino)Benzenes and an Investigation into Their Activity as Catalysts for Carbon-Carbon Bond Formation. Organometallics 2002, 21, 5259-5264. (i) Fossey, J. S.; Richards, C. J. Synthesis of 2,6- Bis(2-Oxazolinyl)Phenylplatinum-(II) NCN Pincer Complexes by Direct Cyclometalation. Catalysts for Carbon-Carbon Bond Formation. Organometallics 2004, 23, 367-373. (j) Nerush, A.; Vogt, M.; Gellrich, U.; Leitus, G.; Ben-David, Y.; Milstein, D. Template Catalysis by Metal-Ligand Cooperation. C-C Bond Formation via Conjugate Addition of Non-Activated Nitriles under Mild, Base-Free Conditions Catalyzed by a Manganese Pincer Complex. J. Am. Chem. Soc. 2016, 138, 6985-6997.

(3) (a) Szabó, K. J. Pincer Complexes as Catalysts in Organic Chemistry. *Top. Organomet. Chem.* **2013**, 40, 203–242. (b) Bhattacharya, P.; Guan, H. Synthesis and Catalytic Applications of Iron Pincer Complexes. *Comments Inorg. Chem.* **2011**, 32, 88–112. (c) Balaraman, E.; Milstein, D. Hydrogenation of Polar Bonds Catalysed by Ruthenium-Pincer Complexes. *Top. Organomet. Chem.* 

2014, 48, 19–44. (d) Werkmeister, S.; Neumann, J.; Junge, K.; Beller, M. Pincer- Type Complexes for Catalytic (De)Hydrogenation and Transfer (De)Hydrogenation Reactions: Recent Progress. *Chem. - Eur. J.* 2015, 21, 12226–12250. (e) Zell, T.; Milstein, D. Hydrogenation and Dehydrogenation Iron Pincer Catalysts Capable of Metal–Ligand Cooperation by Aromatization/Dearomatization. *Acc. Chem. Res.* 2015, 48, 1979–1994. (f) Singleton, J. T. The Uses of Pincer Complexes in Organic Synthesis. *Tetrahedron* 2003, 59, 1837–1857

- (4) (a) Young, K. J. H.; Oxgaard, J.; Ess, D. H.; Meier, S. K.; Stewart, T.; Goddard, W. A., III; Periana, R. A. Experimental Realization of Catalytic CH4 Hydroxylation Predicted for an Iridium NNC Pincer Complex, Demonstrating Thermal, Protic, and Oxidant Stability. Chem. Commun. 2009, 3270-3272. (b) Esteruelas, M. A.; Oliván, M.; Vélez, A. POP-Rhodium-Promoted C-H and B-H Bond Activation and C-B Bond Formation. Organometallics 2015, 34, 1911-1924. (c) Watts, D.; Wang, D.; Adelberg, M.; Zavalij, P. Y.; Vedernikov, A. N. C- H and O 2 Activation at a Pt(II) Center Enabled by a Novel Sulfonated CNN Pincer Ligand. Organometallics 2017, 36, 207-219. (d) Gao, Y.; Guan, C.; Zhou, M.; Kumar, A.; Emge, T. J.; Wright, A. M.; Goldberg, K. I.; Krogh-Jespersen, K.; Goldman, A. S.  $\beta$ -Hydride Elimination and C-H Activation by an Iridium Acetate Complex, Catalyzed by Lewis Acids. Alkane Dehydrogenation Cocatalyzed by Lewis Acids and [2,6- Bis(4,4-Dimethyloxazolinyl)-3,5-Dimethylphenyl]Iridium. J. Am. Chem. Soc. 2017, 139, 6338-6350.
- (5) (a) Crabtree, R. H. Deactivation in Homogeneous Transition Metal Catalysis: Causes, Avoidance, and Cure. Chem. Rev. 2015, 115, 127-150. (b) Archer, A. M.; Bouwkamp, M. W.; Cortez, M.-P.; Emil Lobkovsky, A.; Chirik, P. J. Arene Coordination in Bis(Imino)-Pyridine Iron Complexes: Identification of Catalyst Deactivation Pathways in Iron-Catalyzed Hydrogenation and Hydrosilation. Organometallics 2006, 25, 4269-4278. (c) Volpe, E. C.; Wolczanski, P. T.; Lobkovsky, E. B. Aryl-Containing Pyridine-Imine and Azaallyl Chelates of Iron toward Strong Field Coordination Compounds. Organometallics 2010, 29, 364-377. (d) Chirik, P. J. Iron- and Cobalt-Catalyzed Alkene Hydrogenation: Catalysis with Both Redox-Active and Strong Field Ligands. Acc. Chem. Res. 2015, 48, 1687-1695. (e) Lyaskovskyy, V.; de Bruin, B. Redox Non-Innocent Ligands: Versatile New Tools to Control Catalytic Reactions. ACS Catal. 2012, 2, 270-279. (f) Peters, R. Cooperative Catalysis: Designing Efficient Catalysts for Synthesis; Wiley-VCH: Weinheim, Germany, 2015.
- (6) (a) Hopkinson, M. N.; Richter, C.; Schedler, M.; Glorius, F. An Overview of N-Heterocyclic Carbenes. *Nature* **2014**, *510*, 485–496. (b) Díez-González, S.; Marion, N.; Nolan, S. P. N-Heterocyclic Carbenes in Late Transition Metal Catalysis. *Chem. Rev.* **2009**, *109*, 3612–3676. (c) Schuster, O.; Yang, L.; Raubenheimer, H. G.; Albrecht, M. Beyond Conventional N -Heterocyclic Carbenes: Abnormal, Remote, and Other Classes of NHC Ligands with Reduced Heteroatom Stabilization. *Chem. Rev.* **2009**, *109*, 3445–3478. (d) Herrmann, W. A. N-Heterocyclic Carbenes: A New Concept in Organometallic Catalysis. *Angew. Chem., Int. Ed.* **2002**, *41*, 1290–1309. (e) Charra, V.; de Frémont, P.; Braunstein, P. Synthesis and Reactivity of Metal Complexes Bearing Functional N-Heterocyclic Carbene Ligands. *Coord. Chem. Rev.* **2017**, *341*, 53–176.
- (7) Some examples of pincer NHC complexes: (a) Peris, E.; Crabtree, R. H. Recent Homogeneous Catalytic Applications of Chelate and Pincer N-Heterocyclic Carbenes. *Coord. Chem. Rev.* **2004**, 248, 2239–2246. (b) Morales-Morales, D. *Pincer Compounds: Chemistry and Applications*; Elsevier: Amsterdam, The Netherlands, 2018. (c) Bhattacharya, P.; Guan, H. Synthesis and Catalytic Applications of Iron Pincer Complexes. *Comments Inorg. Chem.* **2011**, 32, 88–112. (d) Gunanathan, C.; Milstein, D. Bond Activation and Catalysis by Ruthenium Pincer Complexes. *Chem. Rev.* **2014**, 114, 12024–12087. A review on iron carbene complexes: (e) Riener, K.; Haslinger, S.; Raba, A.; Högerl, M. P.; Cokoja, M.; Hermann, W. A.; Kühn, F. E. Chemistry of Iron N-Heterocyclic Carbene Complexes: Syntheses, Reactivities, and Catalytic Applications. *Chem. Rev.* **2014**, 114, 5215–5272.

- (8) (a) Matson, E. M.; Espinosa Martinez, G.; Ibrahim, A. D.; Jackson, B. J.; Bertke, J. A.; Fout, A. R. Nickel(II) Pincer Carbene Complexes: Oxidative Addition of an Aryl C—H Bond to Form a Ni(II) Hydride. *Organometallics* **2015**, 34, 399—407. (b) Ibrahim, A. D.; Tokmic, K.; Brennan, M. R.; Kim, D.; Matson, E. M.; Nilges, M. J.; Bertke, J. A.; Fout, A. R. Monoanionic Bis(Carbene) Pincer Complexes Featuring Cobalt(I-III) Oxidation States. *Dalton. Trans.* **2016**, 45, 9805—9811. (c) Reilly, S. W.; Webster, C. E.; Hollis, T. K.; Valle, H. U. Transmetallation from CCC-NHC Pincer Zr Complexes in the Synthesis of Air-Stable CCC-NHC Pincer Co(III) Complexes and Initial Hydroboration Trials. *Dalton. Trans.* **2016**, 45, 2823—2828
- (9) IUPAC. Compendium of Chemical Terminology ("Gold Book"); Compiled by McNaught, A. D.; Wilkinson, A.; Blackwell Scientific: Oxford, U.K., 1997.
- (10) (a) Evans, D. F. The Determination of the Paramagnetic Susceptibility of Substances in Solution by Nuclear Magnetic Resonance. *J. Chem. Soc.* **1959**, 2003–2005. (b) Figgis, B. N.; Lewis, J. The Magnetochemistry of Complex Compounds; In Lewis, J.; Wilkins, R. G. *Modern Coordination Chemistry*; Wiley: New York, 2015.
- (11) (a) Huckaba, A. J.; Hollis, T. K.; Howell, T. O.; Valle, H. U.; Wu, Y. Synthesis and Characterization of a 1,3-Phenylene-Bridged N-Alkyl Bis(Benzimidazole) CCC-NHC Pincer Ligand Precursor: Homobimetallic Silver and Rhodium Complexes and the Catalytic Hydrosilylation of Phenylacetylene. *Organometallics* **2013**, 32, 63–69. (b) Raynal, M.; Cazin, C. S. J.; Vallée, C.; Olivier-Bourbigou, H.; Braunstein, P. A New Stable CNHCCHCNHCN-Heterocyclic Dicarbene Ligand: Its Mono- and Dinuclear Ir(i) and Ir(i)—Rh(i) Complexes. *Dalton. Trans.* **2009**, *0*, 3824–3832.
- (12) (a) Otting, G.; Soler, L. P.; Messerle, B. A. Measurement of Magnitude and Sign of Heteronuclear Coupling Constants in Transition Metal Complexes. *J. Magn. Reson.* **1999**, *137*, 413–429. (b) Bampos, N.; Field, L. D.; Messerle, B. A. Measurement of Heteronuclear Coupling Constants in Organometallic Complexes Using High-Resolution 2D NMR. *Organometallics* **1993**, *12*, 2529–2535.
- (13) Bhattacharya, P.; Krause, J. A.; Guan, H. Iron Hydride Complexes Bearing Phosphinite-Based Pincer Ligands: Synthesis, Reactivity, and Catalytic Application in Hydrosilylation Reactions. *Organometallics* **2011**, *30*, 4720–4729.
- (14) Klawitter, I.; Meyer, S.; Demeshko, S.; Meyer, F. Nickel(II) and Iron(II) Complexes with Tetradentate NHC/Amide Hybrid Ligands. *Z. Naturforsch., B: J. Chem. Sci.* **2013**, *68*, 458–466.
- (15) Coe, B. J.; Glenwright, S. J. Trans-Effects in Octahedral Transition Metal Complexes. *Coord. Chem. Rev.* **2000**, 203, 5–80.
- (16) (a) Camp, A. M.; Kita, M. R.; Grajeda, J.; White, P. S.; Dickie, D. A.; Miller, A. J. M. Mapping the Binding Modes of Hemilabile Pincer-Crown Ether Ligands in Solution Using Diamagnetic Anisotropic Effects on NMR Chemical Shift. Inorg. Chem. 2017, 56, 11141-11150. (b) Kita, M. R.; Miller, A. J. M. Cation-Modulated Reactivity of Iridium Hydride Pincer-Crown Ether Complexes. J. Am. Chem. Soc. 2014, 136, 14519-14529. (c) Gomez-Coca, S.; Cremades, E.; Aliaga-Alcalde, N.; Ruiz, E. Mononuclear Single-Molecule Magnets: Tailoring the Magnetic Anisotropy of First-Row Transition-Metal Complexes. J. Am. Chem. Soc. 2013, 135, 7010-7018. (d) Gómez-Coca, S.; Cremades, E.; Aliaga-Alcalde, N.; Ruiz, E. Huge Magnetic Anisotropy in a Trigonal-Pyramidal Nickel(II) Complex. Inorg. Chem. 2014, 53, 676-678. (e) Rouf, S. A.; Mareš, J.; Vaara, J. Relativistic Approximations to Paramagnetic NMR Chemical Shift and Shielding Anisotropy in Transition Metal Systems. J. Chem. Theory Comput. 2017, 13, 3731-3745. (f) Novikov, V. V.; Pavlov, A. A.; Belov, A. S.; Vologzhanina, A. V.; Savitsky, A.; Voloshin, Y. Z. Transition Ion Strikes Back: Large Magnetic Susceptibility Anisotropy in Cobalt(II) Clathrochelates. J. Phys. Chem. Lett. 2014, 5, 3799-3803. (g) Coste, S. C.; Vlaisavljevich, B.; Freedman, D. E. Magnetic Anisotropy from Main-Group Elements: Halides versus Group 14 Elements. Inorg. Chem. 2017, 56, 8195-8202. (h) Greif, A. H.; Hrobárik, P.; Hrobáriková, V.; Arbuznikov, A. V.; Autschbach, J.;

Kaupp, M. A Relativistic Quantum-Chemical Analysis of the Trans Influence on <sup>1</sup>H NMR Hydride Shifts in Square-Planar Platinum(II) Complexes. *Inorg. Chem.* **2015**, *54*, 7199–7208. (i) Hrobárik, P.; Hrobáriková, V.; Meier, F.; Repiský, M.; Komorovský, S.; Kaupp, M. Relativistic Four- Component DFT Calculations of <sup>1</sup>H NMR Chemical Shifts in Transition-Metal Hydride Complexes: Unusual High-Field Shifts Beyond the Buckingham—Stephens Model. *J. Phys. Chem. A* **2011**, *115*, 5654–5659.

- (17) Martinez, G. E.; Ocampo, C.; Park, Y. J.; Fout, A. R. Accessing Pincer Bis(Carbene) Ni(IV) Complexes from Ni(II) via Halogen and Halogen Surrogates. *J. Am. Chem. Soc.* **2016**, *138*, 4290–4293.
- (18) Gibson, D. H. Carbon Dioxide Coordination Chemistry: Metal Complexes and Surface-Bound Species. What Relationships? *Coord. Chem. Rev.* **1999**, *185*–*186*, 335–355.
- (19) Fong, H.; Peters, J. C. Hydricity of an Fe-H Species and Catalytic CO 2 Hydrogenation. *Inorg. Chem.* **2015**, *54*, 5124–5135.
- (20) Pangborn, A. B.; Giardello, M. A.; Grubbs, R. H.; Rosen, R. K.; Timmers, F. J. Safe and Convenient Procedure for Solvent Purification. *Organometallics* **1996**, *15*, 1518–1520.
- (21) Weitz, I. S.; Rabinovitz, M. The Application of C8K for Organic Synthesis: Reduction of Substituted Naphthalenes. *J. Chem. Soc., Perkin Trans.* 1 1993, 10, 117.